Global fitting and parameter identifiability for amyloid-β aggregation with competing pathways

Pratip Rana*, Priyankar Bose*, Ashwin Vaidya†, Vijay Rangachari‡, and Preetam Ghosh*
*Department of Computer Science, Virginia Commonwealth University, Richmond, VA, United States
†Department of Mathematical Science, Montclair State University, Montclair, NJ, United States
‡Department of Chemistry and Biochemistry, University of Southern Mississippi, Hattiesburg, MS, United States

***Abstract*—Aggregation of the amyloid-β (Aβ) protein has been implicated in Alzheimer's disease (AD). Since, low molecular weight Aβ aggregates are hypothesized to serve as the primary toxic species in AD pathogenesis, significant research has been conducted to understand the mechanistic details of the aggregation process. We previously demonstrated that heterotypic interactions between Aβ and fatty acids (FAs) can lead to competing pathways of Aβ aggregation, termed as the off-pathway; this off-pathway kinetics can also be modulated by FA concentrations as captured by mass action models. We employed ensemble kinetics simulations which uses a system of Ordinary Differential Equations to model the competing on- and off-pathways of Aβ aggregation that were trained and validated by biophysical experiments. However, these models had several rate constants, treated as free parameters to be estimated, which resulted in over-fitting of the model. Hence, in this paper, we present a global fitting based method to accurately identify the rate constants involved in the complex competing pathway model of Aβ aggregation. We additionally employ detailed parameter identifiability tests for uncertainty quantification using the profile likelihood method. Since, the emergence of off- or on-pathway aggregates are typically controlled by a narrow set of rate constants, it is imperative to rigorously identify the proper rate constants involved in these pathways. These rate constants serve as a basis for future experiments on modulating the aggregation pathways to populate a particular possibly less toxic oligomeric species. The obtained rate constants also motivate new biophysical experiments to better understand the mechanisms of amyloid aggregation in other neurodegenerative diseases.**

***Index Terms*—systems biology, profile likelihood, optimization, global fitting, protein aggregation.**

I. Introduction

Aggregation of the amyloid β (Aβ) protein is an important process in Alzheimer disease (AD) pathogenesis. Proteolytic processing of the amyloid precursor protein generates A$\beta(1-40)$ and A$\beta(1-42)$ peptides, which spontaneously aggregate to form insoluble fibrils that deposit as senile plaques in the AD brain. During aggregation, soluble proteins misfold into insoluble fibrils comprising of cross-β-sheets. Fibrils along with smaller oligomers are believed to be the main toxic agents causing synaptic dysfunction and neural loss ([1], [2], [3], [4]). Hence, several studies have focused on understanding the biophysical and biochemical aspects of aggregation.

Aβ aggregation towards fibril formation proceeds along the canonical on-pathway; however, competing partners such as fatty acids (FAs) can shift the oligomer formation to the off-pathway that arrests fibril formation by producing smaller soluble oligomers. We demonstrated that it is possible that the reactions involving Aβ could switch between the on- and off-pathways [5] by changes in FA concentration. Several prior studies also reveal a rate-limiting mechanism for the formation of the nucleus or nuclei in the on-pathway ([6], [7], [8], [9], [10], [11]). The on-pathway reactions typically consist of two phases. The first phase comprises of the nucleation process where the soluble oligomers aggregate at a slower pace, called the lag phase. The second phase is known as the elongation or the fibrillation phase, and is designated by rapid fibril formation. We have earlier explored the heterotypic interactions between Aβ and FAs by using two independent tools: reduced-order modeling (**ROM**) and ensemble kinetic simulations (**EKS**) [12], both of which were based on Ordinary Differential Equations (ODEs). On the other hand, the psuedo-micellar phase in the off-pathway (around the critical micelle concentration, CMC) can be categorized by three different phases [12], [13]. In the first phase, the monomers react with the pseudomicelles to make 4mers. In the next phase, these 4mers elongate (using monomers) to form 12mers. Finally, the 12mers combine with the 4-11mers of the second phase to form 12-23mers. We also assume that switching between on- and off-pathways can occur at any oligomer level. We have established these on- or off-pathway reactions and their switching behavior in our previous work ([5], [12], [14], [15]).

ODEs are widely used to model biological dynamics. A central challenge of ODE models is to estimate the various model parameters such as the concentration of reactants and the rate constants to calibrate the model. This is achieved by optimizing an objective function to evaluate the goodness of fit to the experimental data on aggregation kinetics. The likelihood function, which is analogous to the least-squares criterion in typical Systems Biology applications, is an efficient objective function for this purpose. Another vital step in this modeling procedure is the assessment of uncertainty which is typically done by calculating the confidence interval for the parameters. Standard errors such as, the propagation of measurement uncertainty, are modeled by the Gaussian law of error propagation which is based on the linearization of the model. However, mechanistic models in Systems Biology are typically quite complex and exhibit nonlinear characteristics that cannot be properly captured by such regression models.

The confidence intervals of different parameters may present complex patterns due to the non-linearity in the likelihood function. Here, classical methods may provide rough approxi-

2471-7819/20/$31.00 ©2020 IEEE
DOI 10.1109/BIBE50027.2020.00020

mations for finite samples. In cases of structural and practical non-identifiability [16], this method becomes infeasible. In contrast, the profile likelihood method results in confidence intervals, which do not vary with parameter transformation, and are immune to the nonlinear distortions of the likelihood landscape. Hence, the profile likelihood is a one-dimensional representation indicating the values of a parameter, that statistically agrees with available measurements. Profile likelihood is thus a popular method for calculating confidence intervals and identifiability of parameters in systems biology applications.

In this paper, we use **COPASI** [17] to model the reactions in Aβ aggregation along competing pathways. We estimate the parameters by performing a global fit with experimental results considering separate experiments on individual pathways as well as a comprehensive competing pathways scenario. We also perform uncertainty quantification using COPASI and **PyBNF** [18] by using the profile likelihood method.

II. Related works:

The following works form the skeleton of our framework.

A. *Detailed description of Aβ competing pathways reactions*

Heterotypic interactions between FAs and Aβ were studied in [12] by using two independent methods: reduced order modelling (ROM) and Ensemble Kinetic Simulations (EKS), to validate our prior experimental observations. These models showed the significance of the initial condition and concentration of the species from both pathways in dictating the outcomes of aggregation. Furthermore, [5] introduced a new game theoretic approach using the ROM and EKS methods to model the dynamics of Aβ aggregation; this work established the possibilities of switching of oligomers between the two pathways and also demonstrated control mechanisms that favor the prevalence of oligomers from a particular pathway.

We experimentally demonstrated on- to off-pathway switching in [5]. 5 mM C12 FA was added to 25 μM Aβ42 buffered in 20 mM Tris, 50 mM NaCl at pH 8.0 (*micelle addition event*) in two separate experiments at 3h, 24h. It resulted in increased ThT fluorescence without a lag phase motivating two hypotheses: a) on introducing C12 FA, unreacted monomers adopt off-pathway, and/or b) preformed aggregates along on-pathway are switched back to off-pathway. For off- to on-pathway switching, we incubated 5 mM C12 FA, exhibiting an exponential increase in ThT fluorescence; the sample was then diluted 5- and 10-folds to reduce the effective concentration of C12 FA from 1 to 0.1 mM, which is well below its CMC (*micelle removal event*). When dilution of C12 FA was introduced at 5h and 24h time points, appropriately blank subtracted data showed a sharp rise in ThT fluoresence; this indicated the switching of off- to on- pathway species. The 5- and 10-fold dilutions led to the rise in the molecular weight of the aggregates including the formation of fibrils both at 5h and 24 h as compared to the sample in 5 mM C12 FA.

B. *Parameter Estimation in ODE models:*

Parameter estimation in ODE models is solved as an optimization problem by minimizing an objective function that measures the deviation between simulated and experimental data. Several prior works have developed heuristic global/local search methods for stochastic systems where the embedded noise can introduce errors in the gradient estimation. Derivative free optimization methods avoid computation of derivatives of the objective function making them, in principle, less susceptible to stochastic noise than the gradient-based methods. Our Aβ competing pathways model using the EKS method also needs a gradient-free parameter optimization algorithm as it consists of several biochemical reactions from the competing pathways that makes the gradient-based models less effective.

Optimization algorithms can be classified as deterministic or stochastic. In stochastic optimization, metaheuristics are generally used [19] that solve the optimization problem by guiding and modifying other heuristics to provide better solutions than local optimization algorithms; however, they also involve a tradeoff between randomization and local search. Also, metaheuristics require moderate computation time but may fail in some cases. The two major components of metaheuristics are intensification i.e., focusing search operations in the local region given that a good solution was found in that region, and diversification i.e., generating diverse solutions by performing a global search. A good balance of these two components ensures that the global optimality is achieved when the algorithm converges. Different types of metaheuristics include Simulated Annealing, Genetic Algorithms, Differential Evolution, Bee Algorithms, Tabu Search, Harmony Search, and so on [20].

C. *Parameter Identifiability*

The agreement of experimental data with the observables predicted by the parameterized model is measured by an objective function, which is commonly the weighted sum of squared residuals (SSR, [16]). The parameters are estimated using a maximum likelihood estimator. Considering m number of parameters, the likelihood profile of the i^{th} parameter p_i is LP(p_i) and the fitted parameters are $\hat{p_i}$, for $i = 1, ..., m$.

$$LP(p_i) = min_{p_{j\neq i}}(SSR(p_j)) \tag{1}$$

The likelihood profile for each fitted parameter is calculated by re-optimizing the objective function SSR(p_j) with respect to all other parameters i.e, $p_{j\neq i}$ in the neighborhood of the original estimated parameter value $\hat{p_i}$ [21]. A confidence interval of a parameter tells us that the true value of the parameter is located within this interval with probability, numerically equal to the confidence level. If the re-optimized SSR(p_j) exceeds a specific confidence level within the same range, then the parameter is identifiable. The likelihood contour C_{LC} and likelihood ratio C_{LR} for n data points are calculated as:

$$C_{LC} = \{p : SSR(p) \leq SSR(\hat{p})(1 + \frac{m}{n-m}F^{\alpha}_{m,n-m})\}, or \tag{2}$$

$$C_{LR} = \{p : SSR(p) \leq SSR(\hat{p})e^{X^2_{\alpha}/n}\} \tag{3}$$

where $F^{\alpha}_{m,n-m}$ and X^2_{α} represent the upper α-critical values for the F-ratio and Chi-squared distribution, respectively [22].

The confidence intervals can be asymptotic or a finite sample [16]. Sometimes, the number of parameters in the model are more than the number of data points used for fitting. In such cases, with a dearth of data points, the parameters do not properly rely on the data and are called non-identifiable [16]. Non-identifiable parameters can be in turn structurally non-identifiable, when there arises a redundant parameterization due to the insufficient mapping of internal model states to the observables resulting in infinite confidence intervals. Non-identifiable parameters can also be practically non-identifiable, when the amount and quality of experimental data is insufficient and manifests in an infinite confidence interval.

D. *Parameter Uncertainty*

Uncertainty in parameter estimation occurs when the exact value of the parameter is unknown but bounded at both ends. Parameter uncertainty quantification methods start with an assumed prior probability distribution for each parameter and a likelihood function, and aim to sample the multidimensional posterior probability distribution of the parameters given the data. **PyBNF** provides methods for Bayesian uncertainty quantification of parameter estimates [18] by using Markov chain Monte Carlo with the Metropolis-Hastings algorithm or parallel tempering. **PyBNF** can also quantify the uncertainty of model predictions by performing simulations using the sampled parameter or by bootstrapping the resampling data.

III. Method

We used COPASI for the ODE model, parameter estimation and identifiability study and cross-validated them with PyBNF.

A. *COPASI*

COPASI (COmplex PAthway SImulator) is an open-source software [17] for solving mathematical models of biological processes such as metabolic networks, reaction pathways, regulatory networks, etc. It is helpful in studying biochemical networks as it can perform flexible parameter scans, optimization of arbitrary expressions and parameter estimation using time course and steady-state data simultaneously. COPASI reads and writes SBML files through the libsbml library. We used COPASI to convert our earlier ODE based Aβ competing pathways model with switching reactions into SBML format.

B. *PyBioNetFit (PyBNF)*

Various tools like COPASI, D2D, AMICI and PyBNF can parameterize ODE models [23], [24], [17], [18]. **PyBNF** is a recent method, and was chosen because it can support BioNetGen models where the algorithms are parallelized, making the metaheuristics computationally more efficient.

C. *ODE model of on-off pathway switching*

In order to keep our model simple and prevent overfitting, we considered a *minimal set of reactions* to represent the on-off pathway switching. We use the following notations: A_i represents an on-pathway i-mer, A'_i represents an off-pathway i-mer, L represents pseudo-micelles, F represents the on-pathway oligomers or fibrils, F'_i is an off-pathway oligomer and the total ThT signal is the sum of the on-pathway ThT signal ($signal_{on}$) and the off-pathway ThT signal ($signal_{off}$). As in [25], A_{12} is considered equivalent to F i.e., the nucleus of an on-pathway is 12-mer. In the EKS model, we considered that the switching occurs only for oligomers ranging in size from A_1 to A_{11} while A_{12} is the nucleus. The on-pathway oligomers beyond that fibrillate to on-pathway fibrils, F. Likewise, A'_{12} to A'_{23} are considered as F'_1 as they are smaller off-pathway oligomers which is kinetically trapped and hence, lacks the energy to aggregate further. This model was already validated in [12].

I. Reactions in on pathway: (considering A_{12} as F)

$$A_i + A_1 \underset{k_{nu\_}}{\overset{k_{nu}}{\longleftrightarrow}} A_{i+1}; \forall i \in \{1, 2, ..., 11\}$$
$$F + A_1 \underset{k_{fb\_}}{\overset{k_{fb}}{\longleftrightarrow}} F; \forall i \in \{1, 2, ..., 11\} \quad (4)$$

II. Reactions in off pathway model:

$$4A_1 + L \underset{k_{con\_}}{\overset{k_{con}}{\longleftrightarrow}} A'_4$$
$$A'_i + A_1 \underset{k_{nuf\_}}{\overset{k_{nuf}}{\longleftrightarrow}} A'_{i+1}; \forall i \in \{4, 5, ..., 11\}$$
$$A'_{12} + A'_i \underset{k_{el1f\_}}{\overset{k_{el1f}}{\longleftrightarrow}} F'_1; \forall i \in \{4, 5, ..., 11\}$$

III. On to off switching reaction:

$$A'_i \underset{k_{swi\_}}{\overset{k_{swi}}{\longleftrightarrow}} A_i \quad (5)$$

Flux of on pathway reactions:

$$H_i = k_{nuon}[A_i][A_1] - k_{nuon\_}[A_{i+1}]; \forall i \in \{1, 2, \cdots, 11\}$$
$$I_i = k_{fbon}[A_i][F] - k_{fbon\_}[F]; \forall i \in \{1, 2, \cdots, 11\}$$

Flux of the reactions from off pathway

$$G'_1 = k_{con}[A_1]^4[L] - k_{con\_}[A'_4]$$
$$H'_i = k_{nuoff}[A'_{4+i-1}][A_1] - k_{nuoff\_}[A'_{4+i}]; \forall i \in \{1, 2, \cdots, 8\}$$
$$I'_i = k_{fboff}[A'_{4+i-1}][A'_{12}] - k_{fboff\_}[F'_1]; \forall i \in \{1, 2, \cdots, 8\}$$

Flux of on-off switching reaction:

$$J = k_{swi}[A_4] - k_{swi\_}[A'_4] \quad (6)$$

IV. Result

A. *Parameter Estimation and Identifiability of the on-pathway*

First, we fitted the experimental data of the on-pathway, considering the reactions in Eq. 4. These estimated on-pathway parameters were used to define the parameter ranges in the subsequent steps. We used scatter search optimizer from COPASI to fit the on pathway experimental data and found an excellent fit having sum of squared error (SSE) as 0.13 (Fig. 1(a)). For the lowest objective function, we found k_{fb} is about 400 times higher than k_{nu}. The backward nucleation rate constant $k_{nu\_}$ is only $1-2$ times lower than k_{nu}, while $k_{fb\_}$ is almost $100-200$ times lower than k_{fb}.

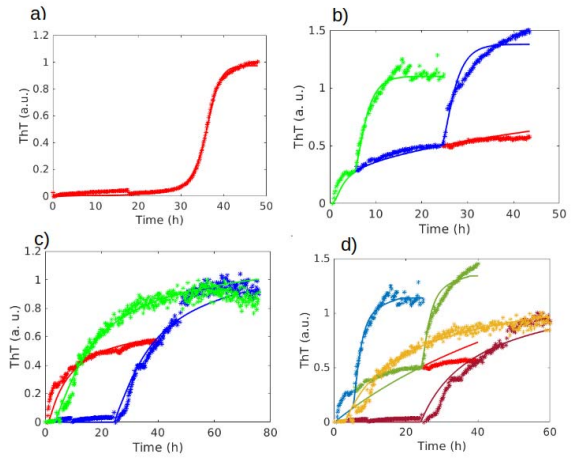

Fig. 1. Fit of EKS models with experimental data from [5]; dots denote experimental data and solid lines are simulated results by EKS. Fit between experimental results and EKS for (a) on-pathway, (b) micelle addition event, (c) micelle removal event and (d) global event considering all the experiments.

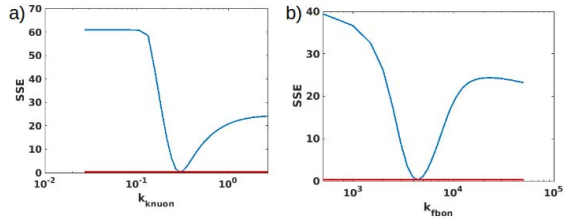

Fig. 2. Parameter identifiability (90% confidence interval) for on pathway.

Next, we calculated the identifiability of the four rate constants of the on-pathway. However, we found the forward rate constants are not identifiable in the presence of backward rate constants, i.e., when the backward rate constants were also considered as free parameters to be estimated. For example, the rate constant k_{nu} is not identifiable in the presence of rate constant $k_{nu\_}$. One explanation for this is that the reaction flux of the nucleation stage can be altered by both forward and backward rate constants. So, we may need concentration data of intermediate species, e.g., A_2, A_3, to properly identify forward rate constant parameters in the presence of the backward rate constants; but, technical limitations and experimental cost is a bottleneck to gather these data. However, we found k_{nu}, and k_{fb} are identifiable when we fixed the corresponding backward rate constants. The profile likelihood of k_{nu} and k_{fb} with fixed backward rate constants, is shown in Fig. 2(a)-(b).

B. Parameter Estimation and Identifiability with the pseudo-micelle addition Event (on-to-off pathway switching)

Next, we fit the pseudo-micelle addition event data from [5]. We built a COPASI model with events at 3h and 24 h, which simulate the addition of pseudo-micelles and monomers

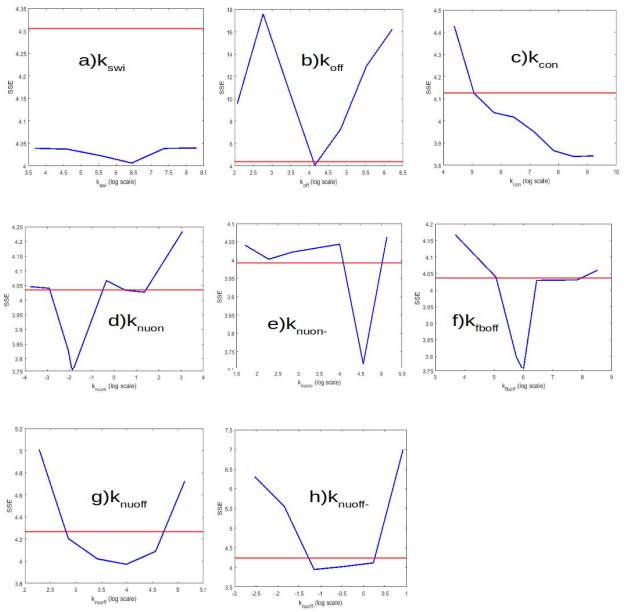

Fig. 3. Parameter identifiability (90% confidence interval) for the micelle addition event.

in the system. Here the on-pathway rate constants are varied between 0.1-10 times of the estimated values from the previous on pathway fit, while all the off-pathway rate constants were varied freely from 10^{-2} to 10^{5} units. The off-pathway mapping constant map' is also varied freely from 10^{0} to 10^{5}. We achieved a good fit between the experimental data and the simulated curve (Fig. 1c). The sum of the squared error (SSE) of the three experiments is 4.12. Here we found that the forward off-pathway nucleation rate constant is quite higher than the forward on-pathway nucleation rate constant. However, the backward rate constant is quite low.

Next, we calculated the profile likelihood of the rate constants using 90% confidence intervals. The parameter identifiability of all the significant parameters of this event (k_{con}, k_{nuoff}, k_{nuoff-}, k_{nuon}, k_{nuon-}, k_{off}, k_{fboff} and k_{swi}) are shown in Fig. 3. The horizontal line cuts the parameter identifiability curve of each parameter at two points: the left and right point of intersection give the lower and upper bounds of the parameter value with 90% confidence, respectively. The parameter value for which the objective function or SSE is minimized lies between these bounds. All the parameters except k_{swi} and k_{con} were found to be identifiable.

C. Parameter Estimation and Identifiability with pseudo-micelle removal event (off-to-on switching)

We next fitted the experimental ThT data for the pseudo-micelle removal event from [5]. We built the COPASI model with all off and on pathway reactions. We also defined an event to simulate micelle removal from the system along with monomer addition. Lastly, we fitted the data using the parameter optimization function of COPASI. Here also, we

Parameters	On-Pathway	On-Off Switching	Off-On Switching	Global
k_{con} $(hr^{-1}\mu M^{-4})$	–	675.528	**139.545**	1221.69
k_{fboff} $(hr^{-1}\mu M^{-1})$	–	**426.503**	**40.3329**	**97.3176**
k_{nuoff} $(hr^{-1}\mu M^{-1})$	–	**28.4215**	**195.943**	**40.8795**
k_{nuoff-} (hr^{-1})	–	**1.41607**	**49.2318**	**8.69222**
k_{nuon} $(hr^{-1}\mu M^{-1})$	22.04	**8.83326**	**4.61013**	**0.141644**
k_{nuon-} (hr^{-1})	12.72	**253.824**	**3.49735**	37.8865
k_{off}	–	**97.024**	**164.59**	–
k_{swi} (hr^{-1})	–	183.97	**0.1**	**2.93977**
k_{off1}	–	–	–	**161.832**
k_{off2}	–	–	–	**48.8039**

TABLE I

PARAMETER VALUES OF THE DIFFERENT MODELS. BOLD DENOTES IDENTIFIABLE PARAMETERS WHILE THE OTHER ONES WERE NOT IDENTIFIABLE.

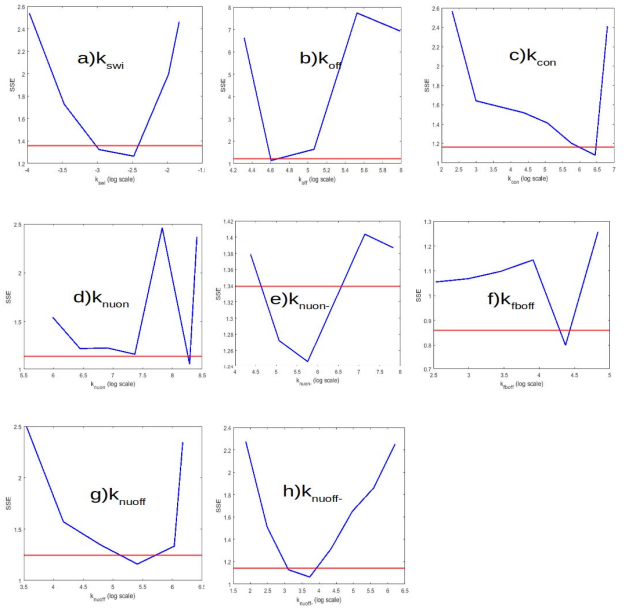

Fig. 4. Parameter identifiability (90% confidence interval) for the micelle removal event.

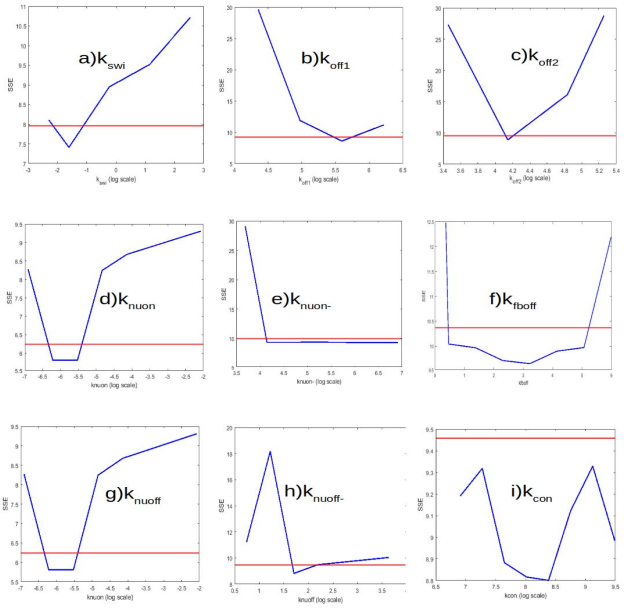

Fig. 5. Parameter identifiability (90% confidence interval) for the global fit.

found an excellent fit with the experimental data (Fig. 1b). The SSE of the fit is just 1.22. We also observed that the ThT intensity was primarily the effect of the off-pathway species. The on-pathway species concentration is quite low to make any significant contributions to the ThT curve. The off-pathway oligomers aggregate with the monomers after the addition event, which eventually causes a sharp increase in the ThT intensity. Moreover, we found that the estimated rate constants of off-pathway are quite similar to those from the previous fit. However, the on-pathway rate constants differed significantly with the previous estimates (from the individual on-pathway fits), and this led us to try a global fit on all the data together. Parameter identifiability of all the significant parameters like k_{con}, k_{nuoff}, k_{nuoff-}, k_{nuon}, k_{nuon-}, k_{off}, k_{fboff} and k_{swi} are shown in Fig. 4. We calculated the profile likelihood of the rate constants using 90% confidence intervals and found all the parameters to be identifiable.

D. Global Fit

We next performed a global fit of all the five curves: on pathway data, micelle addition at 3h and 24 hour, micelle removal at 5h and 24 hour (Fig. 5). We built a COPASI model with two events. The first event simulated the addition of monomer and pseudo-micelles in the system for pseudo-micelle addition event. The second event signifies the micelle removal and addition of monomers in the system. To avoid overfitting, we considered the minimum reaction set of on and off-pathway. We chose the range of parameters carefully using the values estimated from the previous fit. The achieved fit (Fig 1d) had a combined SSE of 8.2. The estimated parameters from the global fit is shown in Table I. Our global fit shows the elongation rate constants (for both off and on-pathways) are quite larger than the nucleation rate constants. However, surprisingly we found that the backward rate constant of the on-pathway is larger than the forward rate constant. The k_{con} rate constant is also found to be quite large.

TABLE II
COMPARISON OF DIFFERENT OPTIMIZATION ALGORITHMS

Algorithm	off-on fit	Time in sec	global fit	Time in sec
Differential Evaluation	1.20	851	52.68	1757
Evolution Strategy (SRES)	1.54	442	68.49	1201
Evolutionary Programming	2.62	67	55.40	245
Genetic Algorithm	8.9	45	76.29	216
Genetic Algorithm SR	3.28	67	69.4	205
Hooke and Jeeves	18.74	452	74	207
Levenberg - Marquardt	97.33	7	93.9	14
Nelder - Mead	82.87	7	59	9.63
Particle Swarm	1.26	1754	53.21	3617
Random Search	4.18	1419	26.19	4488
Scatter search	1.37	333	8.99	674
Simulated Annealing	1.17	10373	72.11	21123
Steepest Descent	346	10	97.34	86
Truncated Newton	357	6	301	21

Lastly, we performed the profile likelihood analysis on these rate constants. Profile likelihood with 90% confidence interval of all significant parameters (k_{con}, k_{nuoff}, k_{nuoff-}, k_{nuon}, k_{nuon-}, k_{off1}, k_{off2}, k_{fboff} and k_{swi}) found all rate constants except k_{con} and $k_{nuon\_}$ are identifiable (Fig 5).

E. Comparison of different optimization methods

We compared fourteen different optimization algorithms in COPASI for two different ODE models (global fit and micelle removal). Three of these algorithms are derivative-based approaches: Levenberg-Marquardt, Steepest Descent, and Truncated Newton, and they performed poorly for both models. The direct search algorithms like Nelder-Mead, Hooke-Jeeves also showed poor performance in both models. The rest of the algorithms are meta-heuristics that performed much better. For the micelle removal event, five different meta-heuristics showed excellent performance, while for the global fit, only one algorithm (scatter search) was able to fit the data. The comparisons of the different algorithms is shown in Table II.

V. CONCLUSION

In this paper, we have performed a global fit and parameter identifiability analysis on the Aβ aggregation dataset. Five different datasets involving different experimental conditions considering the addition and removal of specific reactants at different time-points were fitted to identify the rate constants and parameters that can satisfy each of these five conditions. Moreover, we also performed a parameter identifiability analysis on the model parameters. This method will help the community to estimate the proper rate constants of complex biological models having time-dependent intervention measures in general and identified the correct set of rate constants for the competing pathways model of Aβ aggregation in particular.

Acknowledgement: This work was partially supported by NSF CBET-1802588, 1802793 and 1802641.

REFERENCES

[1] Brett A Chromy, Richard J Nowak, Mary P Lambert, et al. Self-assembly of aβ1-42 into globular neurotoxins. *Biochemistry*, 42(44):12749–12760, 2003.

[2] James P Cleary, Dominic M Walsh, Jacki J Hofmeister, et al. Natural oligomers of the amyloid-β protein specifically disrupt cognitive function. *Nature Neuroscience*, 8(1):79–84, 2005.

[3] Richard O'Brien and Philip Wong. Amyloid precursor protein processing and alzheimer's disease. *Ann. Rev. Neurosc.*, 34:185–204, 2011.

[4] Dominic M Walsh, Igor Klyubin, Julia V Fadeeva, et al. Naturally secreted oligomers of amyloid β protein potently inhibit hippocampal long-term potentiation in vivo. *Nature*, 416(6880):535–539, 2002.

[5] Preetam Ghosh, Pratip Rana, Vijayaraghavan Rangachari, et al. A game theoretic approach to deciphering the dynamics of amyloid-β aggregation along competing pathways. *Royal Society Open Science*, page 191814, 2020.

[6] Alexander K Buell, Céline Galvagnion, Ricardo Gaspar, et al. Solution conditions determine the relative importance of nucleation and growth processes in α-synuclein aggregation. *Proceedings of the National Academy of Sciences*, 111(21):7671–7676, 2014.

[7] Preetam Ghosh, Amit Kumar, Bhaswati Datta, et al. Dynamics of protofibril elongation and association involved in aβ42 peptide aggregation in alzheimer's disease. *BMC Bioinformatics*, 11(S6):S24, 2010.

[8] Samuel Cohen, Sara Linse, Leila Luheshi, et al. Proliferation of amyloid-β42 aggregates occurs through a secondary nucleation mechanism. *Proc. of the Natl. Acad. of Sciences*, 110(24):9758–9763, 2013.

[9] Vijayaraghavan Rangachari, Brenda D Moore, Dana Kim Reed, et al. Amyloid-β (1- 42) rapidly forms protofibrils and oligomers by distinct pathways in low concentrations of sodium dodecylsulfate. *Biochemistry*, 46(43):12451–12462, 2007.

[10] Preetam Ghosh, Bhaswati Datta, and Vijay Rangachari. Computational predictions for the nucleation mass and lag times involved in aβ42 peptide aggregation. In *BIOINFORMATICS*, pages 312–316, 2012.

[11] Srisairam Achuthan, Bong J. Chung, Preetam Ghosh, et al. A modified stokes-einstein equation for aβ aggregation. In *BMC Bioinformatics*, volume 11, page S24. Springer, 2010.

[12] Pratip Rana, Dexter N Dean, Edward D Steen, et al. Fatty acid concentration and phase transitions modulate a β aggregation pathways. *Scientific Reports*, 7(1):1–16, 2017.

[13] Dexter N. Dean, Pratip Rana, Ryan P. Campbell, et al. Propagation of an aβ dodecamer strain involves a three-step mechanism and a key intermediate. *Biophysical Journal*, 114(3):539 – 549, 2018.

[14] Vijayaraghavan Rangachari, Dexter N. Dean, Pratip Rana, et al. Cause and consequence of aβ – lipid interactions in alzheimer disease pathogenesis. *Biochimica et Biophysica Acta (BBA) - Biomembranes*, 1860(9):1652 – 1662, 2018.

[15] Dexter N. Dean, Pradipta K. Das, Pratip Rana, et al. Strain-specific fibril propagation by an aβ dodecamer. *Scientific Reports*, 7(40787), 2017.

[16] Andreas Raue, Clemens Kreutz, Thomas Maiwald, et al. Structural and practical identifiability analysis of partially observed dynamical models by exploiting the profile likelihood. *Bioinformatics*, 25(15):1923–1929, 2009.

[17] Stefan Hoops, Sven Sahle, Ralph Gauges, et al. Copasi—a complex pathway simulator. *Bioinformatics*, 22(24):3067–3074, 2006.

[18] Eshan Mitra, Ryan Suderman, Joshua Colvin, et al. Pybionetfit and the biological property specification language. *IScience*, 19:1012–36, 2019.

[19] Fred Glover. Future paths for integer programming and links to artificial intelligence. *Computers Operations Research*, 13(5):533–549, 1986.

[20] S Ghosh, P Ghosh, K Basu, et al. Gama: an evolutionary algorithmic approach for the design of mesh-based radio access networks. *IEEE Conf. on Local Computer Networks (LCN'05)*, pages 374–381, 2005.

[21] Jörg Schaber. Easy parameter identifiability analysis with copasi. *Biosystems*, 110(3):183–185, 2012.

[22] GAF Seber and CJ Wild. Nonlinear regression new jersey, 2003.

[23] Andreas Raue, Bernhard Steiert, Max Schelker, et al. Data2dynamics: a modeling environment tailored to parameter estimation in dynamical systems. *Bioinformatics*, 31(21):3558–3560, 2015.

[24] Fabian Fröhlich, Barbara Kaltenbacher, Fabian J Theis, et al. Scalable parameter estimation for genome-scale biochemical reaction networks. *PLoS Computational Biology*, 13(1), 2017.

[25] Preetam Ghosh, Ashwin Vaidya, Amit Kumar, et al. Determination of critical nucleation number for a single nucleation amyloid-β aggregation model. *Mathematical Biosciences*, 273:70–79, 2016.